Spectrochimica Acta Part B: Atomic Spectroscopy 236 (2026) 107307

Contents lists available at ScienceDirect

Spectrochimica Acta Part B: Atomic Spectroscopy

journal homepage: www.elsevier.com/locate/sab

Size detection limits in single particle inductively coupled plasma mass spectrometry: Reconsidering the selection of dwell times☆

Isabel Abad-Alvaro, Eduardo Bolea, Francisco Laborda *

Group of Analytical Spectroscopy and Sensors (GEAS), Institute of Environmental Sciences (IUCA), University of Zaragoza, Pedro Cerbuna 12, 50009 Zaragoza, Spain

ARTICLE INFO

Keywords:
Single particle ICP-MS
Dwell time
Size detection limits
Data processing

ABSTRACT

Performance of single particle inductively coupled plasma mass spectrometry (SP-ICP-MS) methods is constrained by the characteristics of the instrumentation. The commercial availability of fast data acquisition quadrupole instruments, which allow the use of dwell times in the microsecond range rather than being restricted to milliseconds, was expected to improve the performance of the technique. When data acquisition frequency is increased, individual particles are recorded as transient signals consisting of multiple-reading events instead of one-reading pulses. Since particle events must be detected above the baseline noise, the highest intensity reading of a transient signal becomes a relevant parameter whose value decreases with decreasing dwell time, as the total intensity of a particle event is independent of the number of readings per event and thus of the selected dwell time. In this work, the effect of dwell time on the attainable size detection limits has been reconsidered, achieving minimum size detection limits when dwell times in the range of 200–500 μs were used, regardless of the baseline level. At such dwell times, particle events from small nanoparticles (e.g., 2–3 times the size detection limit) were recorded within 1–2 readings despite the duration of particle events, which was modified working in both standard and gas reaction modes. Under these conditions, free and proprietary software capable of handling multiple-reading events allowed to process successfully the SP-ICP-MS data independently of the dwell time applied.

1. Introduction

Measurements by inductively coupled plasma mass spectrometry in single particle mode (SP-ICP-MS) require the use of high data acquisition frequencies by applying dwell times in the milli/microseconds range. Particles introduced into the plasma are volatilized, atomized and their atoms ionized to produce a cloud of ions that are extracted through the interface into the mass spectrometer, being detected as individual events if the flow of particles is low enough. With conventional nebulization systems, these flows are achieved by analysing suspensions at low number concentrations [1]. Data recorded must be processed in a convenient way to differentiate readings corresponding to the particle events from those of the baseline, which origin is the background at the mass/charge monitored and dissolved species of the element measured if present, but also to particles below the size critical value [2].

Early SP-ICP-MS methods were based on the use of millisecond dwell times (typically, 3–10 ms) due to constraints of the available commercial instrumentation. Under such conditions, with durations of the particle events in the range of 300–1000 μs, they were recorded as one-reading events (pulses) over a steady baseline. From 2014, instruments allowing dwell times down to 10 μs became commercially available [3,4]. When using dwell times below the duration of particle events, they are recorded as transient signals consisting of several readings. Whereas processing data acquired at millisecond dwell times was relatively easy by using in-house developed spreadsheets [5], as the Single Particle Calculation tool (SPC) proposed by Peters et al. [6], which is freely available (*https://www.wur.nl/en/show/single-particle-calculation-tool.htm*), using microsecond dwell times requires more sophisticated data treatments in line with those used in chromatography. Hence, the new generation of ICP-MS instruments with single particle detection capabilities integrated specific data treatment modules in their software to process these complex signals [5]. With few exceptions [4], proprietary software from vendors lack transparency, although more recently well-documented tools have been developed and are freely available [7,8]

☆ This article is dedicated to John Olesik on the occasion of his 70th birthday and in recognition of his outstanding contributions to both the theory and practice of analytical atomic spectrometry.

* Corresponding author.
E-mail address: *flaborda@unizar.es* (F. Laborda).

https://doi.org/10.1016/j.sab.2025.107307
Received 14 February 2025; Received in revised form 2 July 2025; Accepted 23 August 2025
Available online 24 December 2025

Table 1
Instrumental and data acquisition parameters for SP-ICP-MS.

Parameter	Standard mode	Reaction cell mode
Instrumental parameters		
RF power	1600 W	1600 W
Ar gas flow rate		
Plasma	15 L min^{-1}	15 L min^{-1}
Auxiliary	1.2 L min^{-1}	1.2 L min^{-1}
Nebulizer	1.02 L min^{-1}	1.14 L min^{-1}
Sample flow rate	0.377 mL min^{-1}	0.354 mL min^{-1}
Reaction cell gas flow rate	–	0.5 mL NH_3 min^{-1}
Data acquisition parameters		
Dwell time	5 ms - 25 μs	5 ms - 25 μs
Total acquistion time	60 s	60 s
Isotopes monitored	^{197}Au, ^{107}Ag	^{197}Au

(SPCal at *https://github.com/djdt/spcal* and TOF-SPI at *https://github.com/TOFMS-GG-Group/TOF-SPI*). In the case of SPCal, it is an open-source software that accepts raw data from any type of ICP-MS spectrometer and offers a variety of updated options for data processing [9].

The evolution of data acquisition capabilities in connection with data processing tools may have led to the misconception of considering the use of short microsecond dwell times as the best option in SP-ICP-MS because of an apparent improvement of the signal-to-noise ratio of the detected particle events. Regarding the detection capability for small nanoparticles, when particle events are recorded as one-reading pulses the height of the pulses is independent of the dwell time, whereas for particles events recorded as peaks their height decreases with the dwell time [10]. On the other hand, noise, which is equal to the square root of the baseline intensity in instruments using secondary electron multiplier detectors (quadrupole and double focusing instruments), will decrease as the baseline intensity (measured in counts) decreases with shorter dwell times. As consequence, the size/element mass per particle detection limits tend to decrease with the dwell time for events recorded as pulses, but increase for those recorded as peaks [11]. Hence an optimal dwell time should be expected in the transition region between pulses and peaks. In fact, the use of this region is prone to the so-called split events (detection of a single event in two consecutives pulses) [12] and its use has been discouraged [13]. Under such conditions, the consecutive pulses corresponding to the same particle must be summed up to provide the total intensity of the event and to be recorded as a single particle when data are processed as pulses, by using spreadsheets [12] or other tools [8]. However, two consecutive pulses can be managed as a single peak by the adequate software, regardless of the number of readings when recording particle events, as consequence.

As discussed above, detection of particles in SP-ICP-MS depends not only on the sensitivity of the instrument but also on acquisition conditions as well as data processing, being linked to the duration of the particle events. Durations of several hundreds of microseconds have been reported by different authors [14–18]. The duration of particle events is associated with the formation of the ion cloud and its diffusion along the plasma and depends on the plasma conditions, as well as those of the collision/reaction cell conditions if used [18], the nature of the particle [17] and its size [16,17,19] and shape [16]. For spherical nanoparticles, the duration of the events is proportional to their diameter [16,17,19] if particles are fully detected.

In view of all the issues discussed above, the objective of this work is the re-evaluation of the effect of dwell time on the size/element mass per particle detection limits achievable in SP-ICP-MS. Although most of the study is performed in the so-called standard mode with baselines close to zero, the broadening effect occurring when working in gas reaction/collision mode is also considered, as well as the effect of increasing baseline intensity by adding dissolved analyte. Finally, the role of data processing software when using different dwell times is also considered.

2. Experimental

2.1. Instrumentation

A Perkin-Elmer NexION 2000B mass spectrometer (Toronto, Canada) was used for ICP-MS measurements in single particle mode. The sample introduction system consisted of a glass concentric nebulizer and a baffled cyclonic spray chamber (Meinhard). Default instrumental and data acquisition parameters are listed in Table 1.

2.2. Standards

Diluted suspensions of gold and silver nanoparticles were prepared from commercially available suspensions. Monodisperse citrate-stabilized gold nanoparticles of nominal diameters 10.3 ± 0.9, 18.0 ± 1.8 and 51 ± 5 nm were obtained from nanoComposix (San Diego, CA, USA). LGCQC5050 citrate-stabilized AuNP of nominal diameter 30 nm was obtained from LGC Limited (Teddington, UK). Suspensions of monodisperse citrate-stabilized silver nanoparticles of nominal diameter 41 ± 5 nm was purchased from nanoComposix.

Aqueous gold and silver solutions were prepared from standard stock solutions of 1000 mg L^{-1} (Sigma Aldrich, Switzerland) by dilution in ultrapure water.

2.3. Procedures

Standard suspensions. Dilutions of the stock suspensions of gold and silver nanoparticles were prepared in ultrapure water (Milli-Q Advantage, Molsheim, France) by accurately weighing (± 0.1 mg) aliquots after 1 min sonication. After dilution and before each analysis, the suspensions were bath sonicated for 1 min. Longer sonication times were not used to avoid excessive heating of the suspensions.

SP-ICP-MS measurements. Suspensions were measured in single particle mode using the Syngistix Nano-Application module version 3.2 (PerkinElmer Inc.). The dwell times used were in the range from 5 ms to 25 μs, with total acquisition times of 60 s and recording from 12,000 (at 5 ms) up to 1.5 million (at 25 μs) readings per time scan, respectively (Table 1). Nebulization efficiency was determined using LGCQC5050 Au nanoparticles. Sample flow rate was measured daily gravimetrically.

Recorded signals were exported and processed with the SPCal software version 1.3.3 using the Poisson filter with the Currie option for calculation of the gross critical value (Y_C):

$$Y_C = Y_B + z_{1-\alpha}\sqrt{\eta\, Y_B + \varepsilon} \quad (1)$$

where Y_B is the mean baseline intensity in counts, $z_{1-\alpha}$ denotes the $(1-\alpha)$ quantile of the standard normal distribution, η is a parameter that reflects the ratio of background and sample replicates when paired experiments and net signals are used [20,21], and ε is a correction term for estimation of the baseline variance, which ranges from 0 to 1 [21]. Since gross baseline signals were used for calculation of critical values, η=1 was considered. An ε value of 1 was applied since it has been proposed for low background signals (<10 counts) [22]. The quantile $z_{1-\alpha}$ and hence α, the probability of false positives in a standard normal distribution, were selected to avoid the occurrence of false positives arising from the measured baseline distribution [11]. A $z_{1-\alpha} = 5$ ($\alpha = 2.87 \times 10^{-7}$) was selected by default, although for background signals below 0.1 counts $z_{1-\alpha} = 3$ ($\alpha = 1.35 \times 10^{-3}$, Y_C=3 counts) also allowed to remove successfully any false positive. Since exported data from Syngistix consisted of real numbers (e.g., 23.000019), they were truncated to the corresponding integers before processing with SPCal. Recorded signals were also processed by using the software provided by the manufacturer (Syngistix Nano-Application module version 3.2), applying the same critical values provided by SPCal.

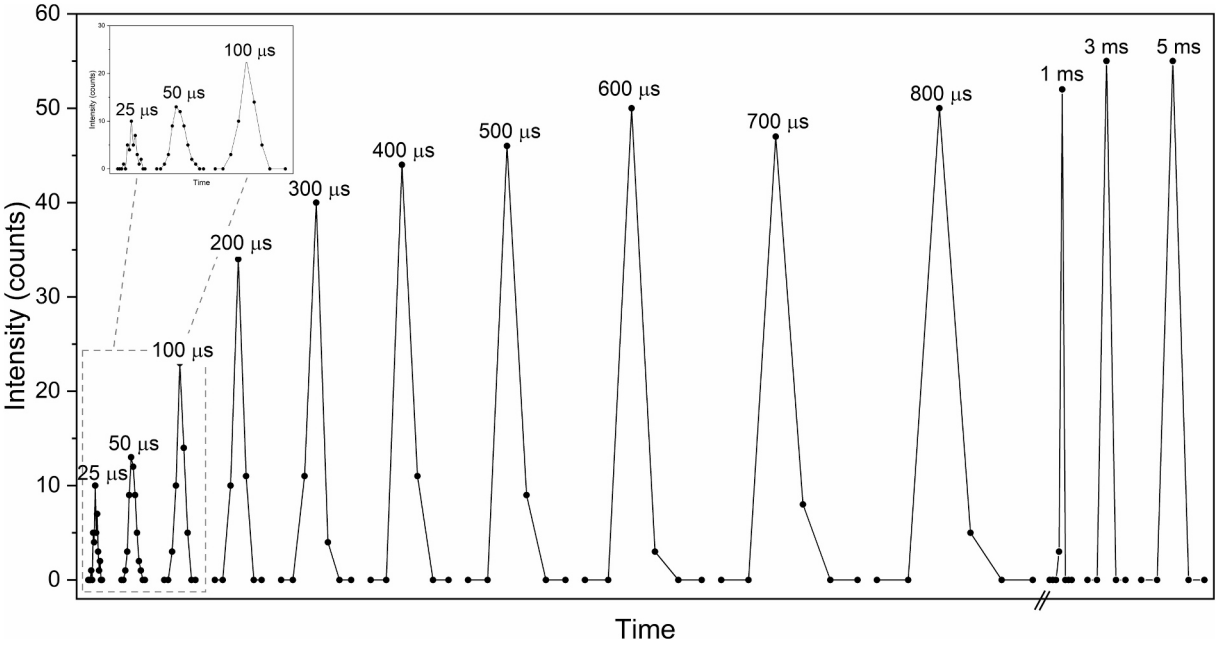

Fig. 1. Profiles of transient signals from 30 nm Au nanoparticles recorded at dwell times from 25 µs up to 5 ms in standard mode. Time scale for 25–800 µs: x10.

2.4. Calculation of size detection limits

Considering that the detection limit is an a priori validation parameter for comparison purposes that involves both type I or α (false positives) and type II or β (false negatives) errors [23], size detection limits (X_D^{size}) were calculated according to a 5-sigma criterion, where $\alpha = 2.87 \times 10^{-7}$ and $\beta = 0.5$. Although this approach involves a *50 %* probability of false negatives, its validity for detection of particles has been proved previously in SP-ICP-MS [11] [24]. Moreover, since detection of particle events over the baseline noise depends on the highest reading recorded along a particle event, the following expression was used:

$$X_D^{size} = \left(\frac{5\,\sigma_B}{K_d'}\right)^{1/3} \quad (2)$$

where σ_B is the standard deviation of the baseline and K_d' the slope of a size calibration ($S_{P\,max} = K_d'\,d^3$) involving the diameter of the spherical particles (d) and the net maximum intensity of the particle events ($S_{P\,max}$). For particle events recorded as one-reading pulses $S_{P\,max}$ is equal to the net intensity of the particle events ($S_P = Y_P - Y_B$, where Y_P is the gross intensity of the reading and Y_B is the mean intensity of the baseline). For particle events recorded as more than one reading (both peaks recorded at microsecond dwell times and split pulses recorded at low milliseconds) $S_{P\,max}$ corresponds to the highest reading along the recorded particle event.

2.5. Estimation of particle event duration

The apparent duration of particle events was estimated from the number of readings along the event multiplied by the dwell time. SPCal v.1.3.3 provides such estimation when selecting in Advanced

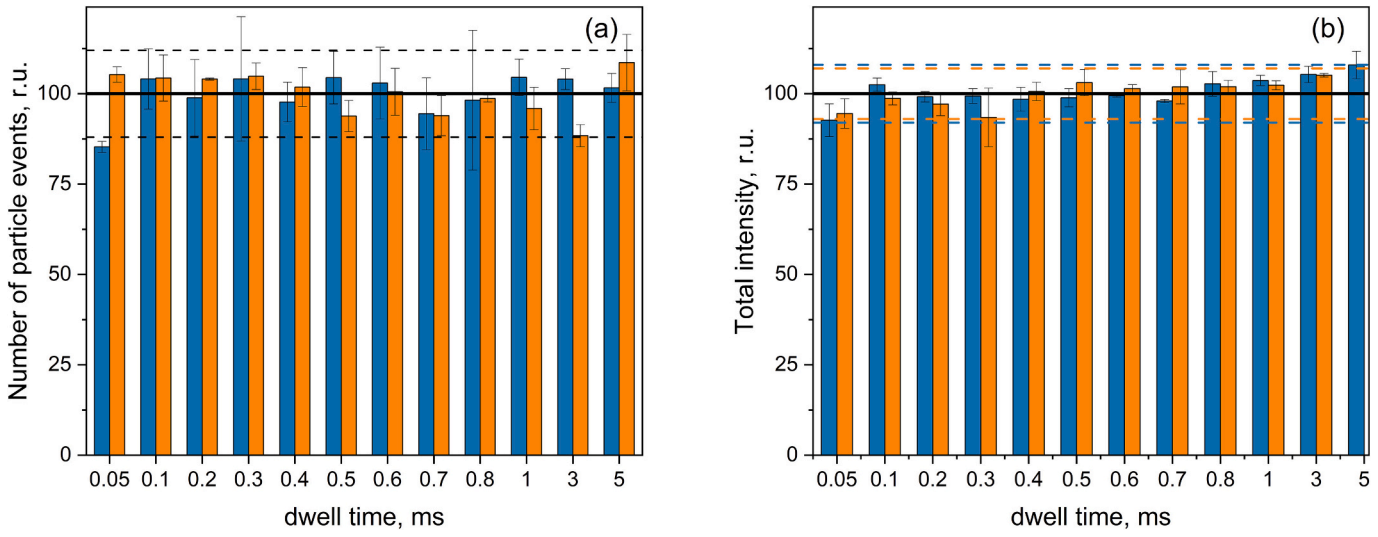

Fig. 2. Normalized number of particle events detected (a) and total intensity of particle events at different dwell times (b). 30 nm Au nanoparticles measured in standard (blue) and gas reaction (orange) modes. Dot lines correspond to the average value uncertainties (as 2-sigma). Data shown processed with SPCal software. *(For interpretation of the references to colour in this figure legend, the reader is referred to the web version of this article.)*

thresholding options "Signal mean" as accumulation method and 1 point for peak detection. This approach considers any reading above the baseline regardless if it is lower or equal to the critical value. In any case, the approach overestimates the actual duration in one dwell time due to the random arrival of the ion clouds to the detector, as explained in the Supplementary Information. Actual durations, independent of dwell time, are obtained by subtracting one dwell time to the widths reported by SPCal in "Peak properties".

3. Results and discussion

3.1. Detection of particle events with respect to dwell time

Fig. 1 shows typical profiles of particle events recorded at dwell times in the range of 5 ms to 25 μs, from suspensions of 30 nm gold nanoparticles under the experimental conditions described in Table 1 (standard mode). When working at 5 and 3 ms dwell times, most of the events were recorded in one reading, whereas from 1 ms to 400 μs, two readings were recorded per event and three for dwell times of 300 and 200 μs (Fig. 1). For dwell times below 200 μs, the higher time resolution selected allowed to obtain better defined peaks, recorded by 5 or more readings. In SP-ICP-MS, the dwell time selected controls the number of readings according to the duration of the particle event. Peak widths (measured as the number of readings multiplied by the dwell time) in the range of 300–500 μs have been reported for this type of nanoparticles under standard mode conditions and 20 μs time resolution [16,17,19], which are in agreement with the event duration independent on dwell time obtained in this work for 30 nm Au nanoparticles (400 μs).

Whereas 1-reading events can be handled directly as pulses, 2-reading events (as happens when using short millisecond dwell times (e.g. 1 ms but also 3 ms) would be considered as two consecutive pulses of lower intensity that should be summed up to give one single pulse of the equivalent intensity [8,12,14]. This is also the case when working at dwell times at which particle events are recorded with two readings (down to 400 μs in the case shown in Fig. 1). However, last generation spectrometers are focused on reducing dwell times to the microsecond range (≤ 100 μs), demanding faster electronics to store larger amounts of data and more complex tools for their processing, requiring peak-based approaches for their processing. In this case, peak-based tools should be able to deal correctly with particle events regardless of the dwell time and their number of readings.

Fig. 2a shows the number of particle events detected from the same suspension of gold nanoparticles at the different dwell time tested. Since high number concentrations must be avoided when applying long dwell times in the range of several milliseconds to reduce the recording of multiple particle events [10], a relatively low number concentration was selected to provide unbiased result in the whole range of dwell times studied. Raw data were processed with the software SPCal, as described in the Experimental Section. Since the average baseline intensity was around 20 counts per second, baseline intensities were in the range of 0.01–0.2 counts depending on the dwell time selected. For the sake of harmonization, an α value of 2.87×10^{-7} ($z_{1-\alpha} = 5$) was initially selected (Y_C=6 counts), although due to the low background signals $z_{1-\alpha} = 3$ ($\alpha = 1.35 \times 10^{-3}$, Y_C=3 counts) also removed all readings from the baselines at the dwell times tested. Similar results were obtained when such critical values were applied with the Syngistix software. In any case, the detection of the complete signal distribution of the nanoparticles was not affected by the threshold applied and the number of events detected was similar and independent of the dwell time, as it can be seen in Fig. 2a.

Fig. 2b shows the normalized mean total net intensity of the particle events recorded at different dwell times by using the processing conditions described above. The total intensity was obtained by summing up the net intensities of the individual readings involved, showing good agreement between the different dwell times tested. The agreement in both number of events and total net intensities at different dwell times, from milli to microseconds, confirms that both peak-based software tested processed SP-ICP-MS data conveniently, which would not have been the case with pulse-based tools.

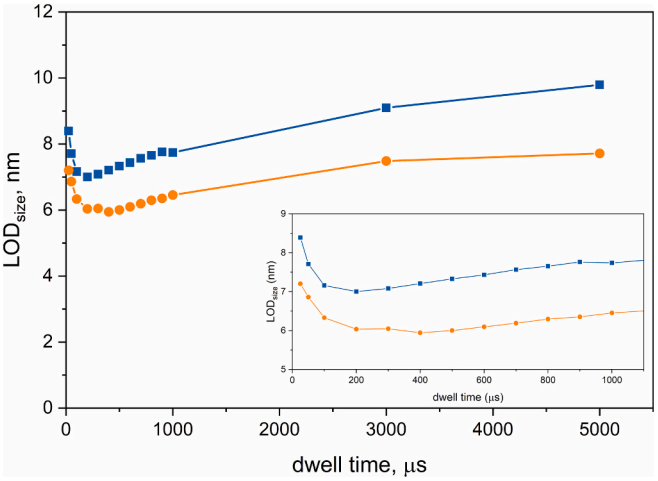

Fig. 3. Size detection limits for Au nanoparticles with respect to dwell time in standard (blue) and gas reaction (orange) modes. *(For interpretation of the references to colour in this figure legend, the reader is referred to the web version of this article.)*

3.2. Size detection limits with respect to dwell time

Detection of particle events over a baseline depends on the noise of the baseline and the maximum intensity (height) of the events and not on their total intensity. As it can be seen in Fig. 1, the height of the events remained fairly constant for dwell times down to 3 ms since most events were recorded as one-reading events, whereas it decreased linearly from 100 μs, when events were recorded as multiple-readings peaks (Fig. 1 of Supplementary Information). As explained above, when dwell times were selected in the range of 1 ms to 200 μs, poorly defined transient signals were obtained with 2–3 readings measured per event.

The baseline intensity expressed in counts is directly proportional to the dwell time and its noise is equal to the square root of its intensity, when it is governed by Poisson statistics, which is the case for spectrometers equipped with secondary electron multiplier detectors at low baseline intensities (Y_B <10 counts). Since size detection limits are proportional to the ratio between the baseline noise and the inverse of the maximum intensity of the particle event (Eq. 2), when decreasing dwell times, size detection limits will decrease if events are recorded as one-reading pulses (3–5 ms) but will increase when recorded as multiple-readings peaks (≤ ca.100 μs), as previously reported [11]. Hence, a minimum should be expected in the transition region of 0.1–3 ms for the cases shown in Fig. 1.

Size detection limits were calculated from Eq. (2). K'_d was estimated at each dwell time from the median net height ($S_{P\,max}$) obtained for the measured nanoparticles, whereas the same baseline count rate (R_B = 20 cps) was considered for the calculations at the different dwell times to avoid additional sources of variability, with $\sigma_B = \sqrt{R_B\, t_{dwell}}$. Fig. 3 shows the variation of size detection limits with respect to dwell time. As expected, size detection limits below 8 nm were obtained for dwell times from 1 ms down to 50 μs, with a minimum size detection limit of 7.0 nm at 200–300 μs.

The effect of the dwell time on the capability of detecting nanoparticles close to the size detection limit is clearly shown when 10 nm Au nanoparticles were measured. Fig. 4 shows the time scans obtained in a range of dwell times between 25 and 1000 μs. It is observed that the number of nanoparticles detected over the critical value clearly decreases when using dwell times shorter than of 200–1000 μs, confirming

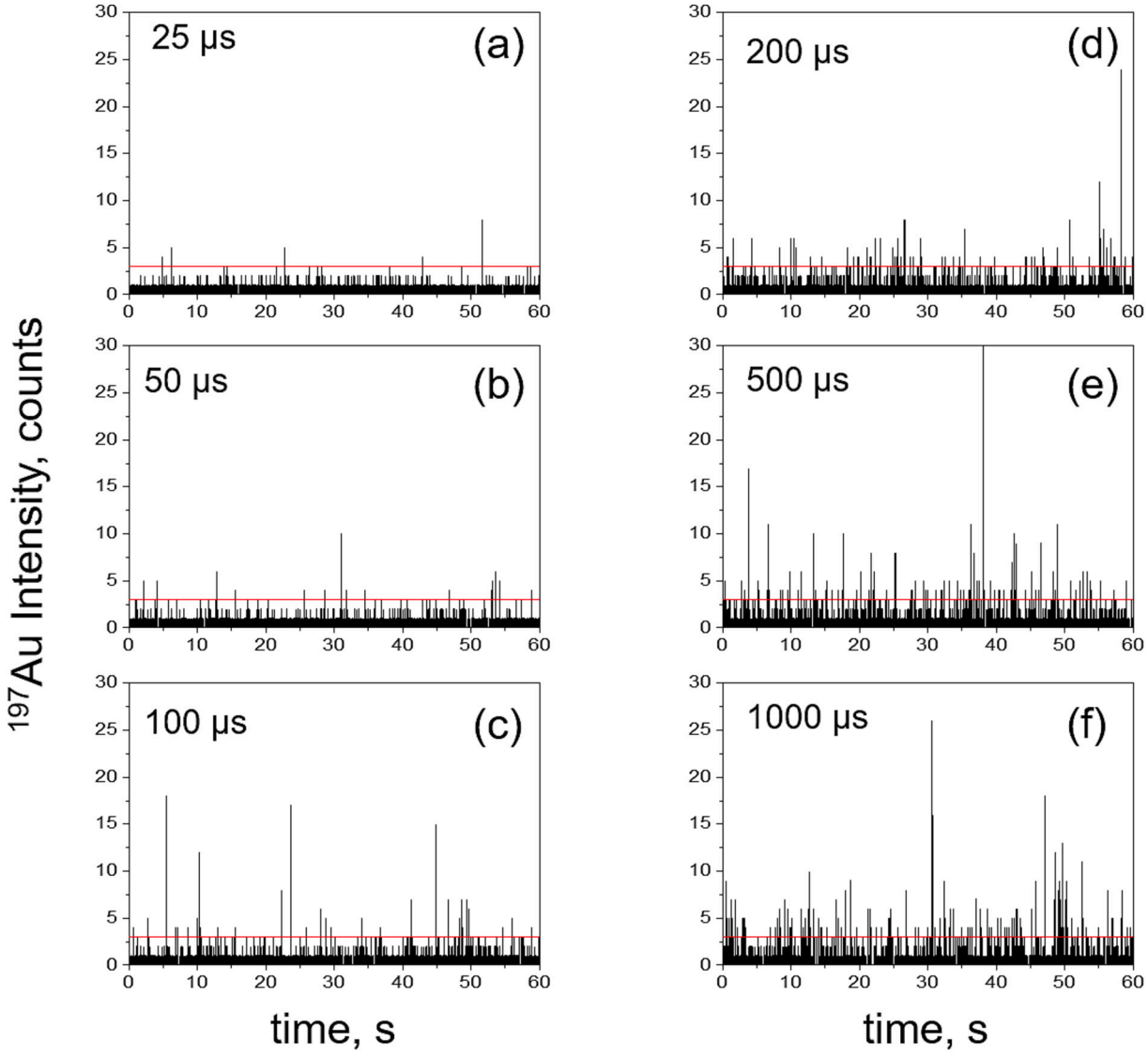

Fig. 4. Time scan of 10 nm Au nanoparticles recorded in standard mode at dwell times of (a) 25, (b) 50, (c) 100, (d) 200, (e) 500 and (f) 1000 µs. Red line: critical value applied for discrimination of baseline and particle readings (3 counts). Concentration: 9.2×10^7 L^{-1}. Number of events detected (mean ± standard deviation; $n = 3$): (a) 7 ± 3, (b) 18 ± 4, (c) 29 ± 3, (d) 61 ± 4, (e) 87 ± 12 and (f) 131 ± 5. *(For interpretation of the references to colour in this figure legend, the reader is referred to the web version of this article.)*

that small nanoparticles close to the size detection limits are hardly detected at such short dwell times in agreement with the size detection limits estimated previously. Similarly, Fig. 5 shows that, despite 20 nm Au nanoparticles were successfully detected using dwell times in the range of 25 to 1000 µs, the size distributions were better defined when using dwell times of 200–500 µs.

These results show that better performance was obtained for small nanoparticles when recording particle events at dwell times of 200–500 µs after the appropriate processing using a peak-based tool. In any case, the duration of the particle events, which depends not only on nanoparticle dimensions, but also on the plasma conditions, as well as the extraction and transport of the ion clouds in the spectrometer, should also be considered on the selection of the optimal dwell time.

3.3. Effect of the duration of particle events and dwell time on size detection limits

To study the effect of the duration of particle events on the behaviour of size detection limits with respect to dwell time, experiments similar to those described above were performed by introducing ammonia in the reaction cell of the spectrometer and applying the instrumental conditions listed in Table 1 (gas reaction mode). Under such conditions, particle events from 30 nm Au nanoparticles showed broader profiles, with durations around 700 µs. In any case, determination of the number and total intensities of particle events recorded at different dwell times lead to similar conclusions than those obtained in standard mode, as it is shown in Fig. 2. Regarding the maximum height of the particle events (Fig. 1 of Supplementary Information) a similar behaviour was observed, although 3-fold improvement on sensitivity was observed when using ammonia. Again, minimum size detection limits at dwell times of 200–500 µs were obtained (Fig. 3), similar to the range obtained in standard mode (200–300 µs), although longer dwell times can be used without increasing size detection limits, due to the broader particle events obtained in the presence of ammonia.

The results obtained confirms that attainable detection limits do not depend only on the dwell time selected, but also on the duration of the particle events which varies with instruments and the experimental conditions selected and should be considered accordingly. In any case, minimum size detection limits are achieved by using the shortest dwell times that allows the particle events to be recorded within 1–2 readings.

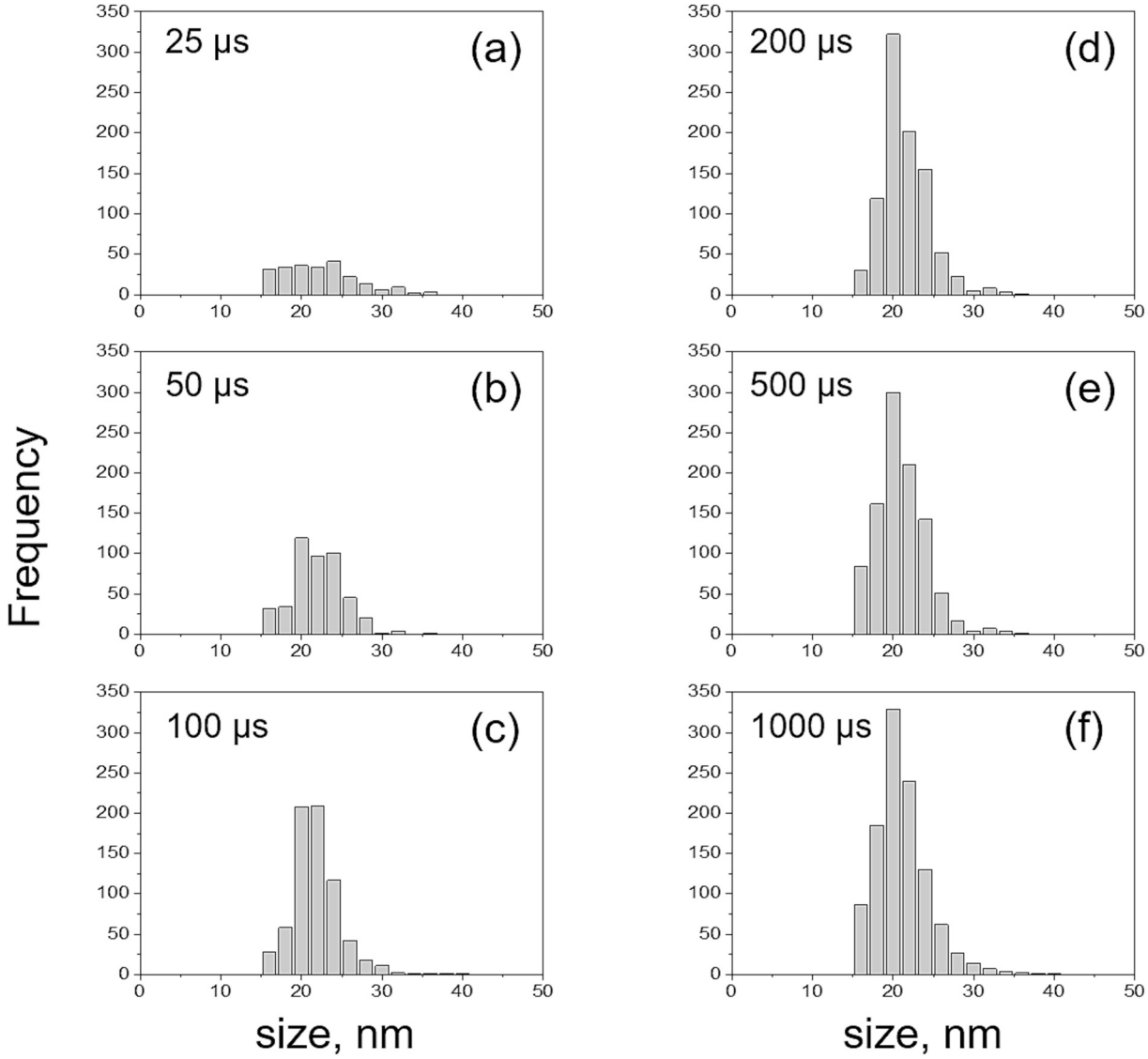

Fig. 5. Size distributions of 20 nm Au nanoparticles recorded in standard mode at dwell times of (a) 25, (b) 50, (c) 100, (d) 200, (e) 500 and (f) 1000 µs. Concentration: 1.0×10^8 L^{-1}.

3.4. Impact of the baseline intensity on size detection limits

The noise of the baseline affects directly to the detectability of particle events through its standard deviation (Eq. 2), which in turn depends on its intensity. As discussed above, reduction of the dwell time implies a decrease of the baseline intensity in counts and hence of its standard deviation, affecting size detection limits in different ways depending on how particle events are recorded. For an ICP-MS instrument, equipped with a secondary electron multiplier detector, a Poisson behaviour is expected at low baseline intensities (< 10 counts) and $\sigma_B = \sqrt{Y_B}$, whereas at higher intensities the contribution of flicker noise must be considered and σ_B should be described as [25]:

$$\sigma_B = \sqrt{Y_B + \xi^2 Y_B^2} \tag{3}$$

where ξ is the flicker noise coefficient. This means that measuring isotopes with high background levels or suspensions with relevant levels of dissolved species of the element monitored, a degradation of size detection limits will be expected in comparison with the behaviours discussed in previous sections, a situation that should be further aggravated when dwell times in the millisecond range are used. This issue has been pointed out in previous publications [10] [13], which has led to the use of microsecond dwell times as an alternative to dilution of samples containing high levels of dissolved elements when measuring at millisecond dwell times.

When ionic silver solutions were measured in single particle mode to handle different baseline levels, the variation of the baseline standard deviation with its intensity was in very good agreement with Eq. 3

Table 2
Size detection limits for Ag nanoparticles with respect to dwell time in ultrapure water and in the presence of dissolved silver (I) (0.5 µg L^{-1}).

Dwell time µs	ultrapure water		0.5 µg L^{-1} Ag(I)		
	Mean baseline intensity counts	X_D^{size} nm	Mean baseline intensity counts	X_D^{size} nm	Nanoparticle recovery %
50	0.0255	17.1	1.19	30.9	95 ± 5
100	0.0483	15.9	2.57	30.6	103 ± 4
200	0.0912	15.3	4.73	29.6	111 ± 5
500	0.226	15.9	11.7	31.1	102 ± 4
1000	0.445	17.3	23.2	33.2	98 ± 5
5000	2.17	21.9	120	36.2	12 ± 2

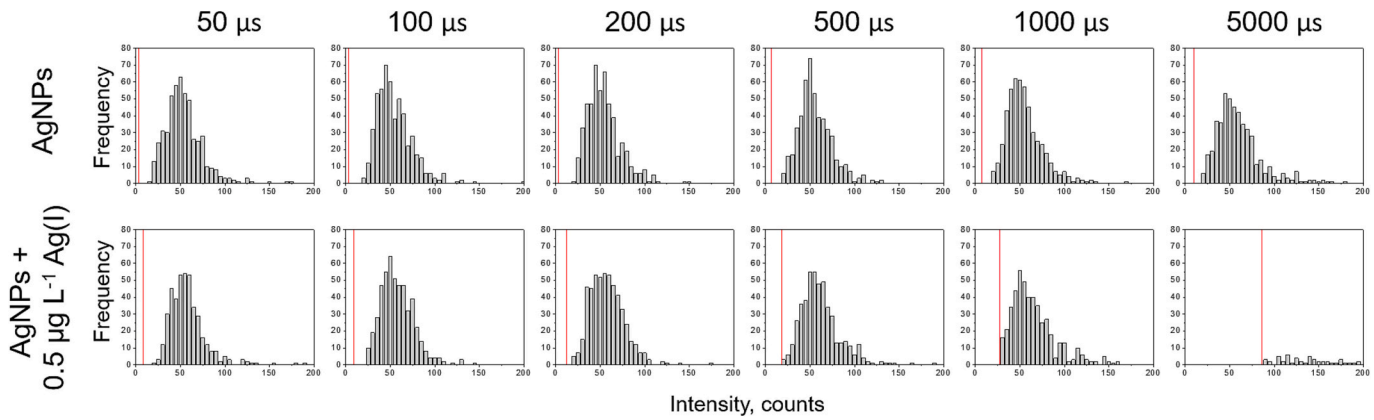

Fig. 6. Intensity distributions of 40 nm Ag nanoparticles in ultrapure water and 0.5 µg L^{-1} of Ag(I) recorded at dwell times of 50–5000 µs. Red line: critical value applied for discrimination of baseline and particle readings Concentration: 2.8×10^7 L^{-1}. *(For interpretation of the references to colour in this figure legend, the reader is referred to the web version of this article.)*

(Fig. S2 of Supplementary Information). Moreover, a decrease in the flicker noise coefficient with dwell time was observed (Table S1 of Supplementary Information) because of its role as a high-frequency cut-off filter, eliminating frequencies greater than twice its inverse [26].

Despite the lower flicker noise at larger dwell times, size detection limits estimated by using the baseline standard deviation calculated from Eq. 3, using the flicker noise coefficients previously calculated, (table S1 of Supplementary Information), showed a similar behaviour for different baseline levels, maintaining the minimum detection limits in the region of several hundreds of microseconds (Table 2). These results confirm that using such dwell times is recommended even at high baseline intensities, as it can be seen in Fig. 6, where the intensity distributions from 40 nm Ag nanoparticles were fully recorded and quantitatively recovered by using dwell times up to 200 µs, which was not the case when using 1 or 5 ms. In any case, the use of short dwell times allows to reduce the baseline intensity and improve size detection limits, although this benefit is lost at very short dwell times.

4. Conclusions

Fast data acquisition in SP-ICP-MS by using short dwell times below 100 µs offers a number of advantages over the use of dwell times of several milliseconds (e.g., longer number concentration dynamic ranges, feasibility of monitoring more than one isotope in the same particle when using quadrupole spectrometers, or avoiding dilution of samples containing high levels of dissolved element) but should not be associated to lower size detection limits. This study has confirmed that the lowest size detection limits are achieved when using dwell times in the range of 200–500 µs, since the maximum height of the particle events, which is the basis of their detectability, decreases when decreasing dwell times but it is not compensated by the decrease of the baseline noise. Under such conditions, particles events can be recorded within 2–3 readings but can be accurately processed by using available peak-based software. Ultimately, the number of readings per event is a function of the event duration, which in turn depends on the size/mass of the element per particle, but also on the instrumental conditions (e.g., the use of a reaction/collision gas). The expected degradation of size detection limits with increasing baseline intensities (e.g., high level of dissolved element) does not affect to these conclusions.

CRediT authorship contribution statement

Isabel Abad-Alvaro: Writing – review & editing, Investigation, Data curation. **Eduardo Bolea:** Writing – review & editing, Supervision, Funding acquisition. **Francisco Laborda:** Writing – original draft, Supervision, Funding acquisition, Conceptualization.

Declaration of competing interest

The authors declare that they have no known competing financial interests or personal relationships that could have appeared to influence the work reported in this paper.

Acknowledgements

This work was funded by the Spanish Ministry of Science and Innovation (MCIN/AEI/*10.13039/501100011033*), project PID2021-123203OB-I00, "ERDF A way of making Europe" and the Government of Aragon, project E29_23R. I.A. thanks the European Union-Next Generation EU and the Spanish Ministry of Universities for funding under the María Zambrano Grant (MZ-240621). Authors would like to acknowledge the use of Servicio General de Apoyo a la Investigación-SAI, Universidad de Zaragoza.

Appendix A. Supplementary data

Supplementary data to this article can be found online at https://doi.org/10.1016/j.sab.2025.107307.

Data availability

Data available on request.

References

[1] F. Laborda, I. Abad-Álvaro, M.S. Jiménez, E. Bolea, Catching particles by atomic spectrometry: *b*enefits and limitations of single particle - inductively coupled plasma mass spectrometry, Spectrochim. Acta Part B At. Spectrosc. 199 (2023) 106570, https://doi.org/10.1016/j.sab.2022.106570.

[2] S.G. Bevers, C. Smith, S. Brown, N. Malone, D.H. Fairbrother, A.J. Goodman, J. F. Ranville, Improved methodology for the analysis of polydisperse engineered and natural colloids by single particle inductively coupled plasma mass spectrometry (spICP-MS), Environ. Sci. Nano 10 (2023) 3136–3148, https://doi.org/10.1039/d3en00425b.

[3] A. Hineman, C. Stephan, Effect of dwell time on single particle inductively coupled plasma mass spectrometry data acquisition quality, J. Anal. At. Spectrom. 29 (2014) 1252–1257, https://doi.org/10.1039/C4JA00097H.

[4] P. Shaw, A. Donard, Nano-particle analysis using dwell times between 10 µs and 70 µs with an upper counting limit of greater than 3 × 10 7 cps and a gold nanoparticle detection limit of less than 10 nm diameter, J. Anal. At. Spectrom. 31 (2016) 1234–1242, https://doi.org/10.1039/C6JA00047A.

[5] M.I. Chronakis, B. Meermann, M. von der Au, The evolution of data treatment tools in single-particle and single-cell ICP-MS analytics, Anal. Bioanal. Chem. (2024) 7–13, https://doi.org/10.1007/s00216-024-05513-4.

[6] R. Peters, Z. Herrera-Rivera, A. Undas, M. Van Der Lee, H. Marvin, H. Bouwmeester, S. Weigel, Single particle ICP-MS combined with a data evaluation tool as a routine technique for the analysis of nanoparticles in complex matrices, J. Anal. At. Spectrom. 30 (2015) 1274–1285, https://doi.org/10.1039/c4ja00357h.

[7] T.E. Lockwood, R. Gonzalez De Vega, D. Clases, An interactive Python-based data processing platform for single particle and single cell ICP-MS, J. Anal. At. Spectrom. 36 (2021) 2536–2544, https://doi.org/10.1039/d1ja00297j.
[8] A. Gundlach-Graham, S. Harycki, S.E. Szakas, T.L. Taylor, H. Karkee, R. L. Buckman, S. Mukta, R. Hu, W. Lee, Introducing "time-of-flight single particle investigator" (TOF-SPI): a tool for quantitative spICP-TOFMS data analysis, J. Anal. At. Spectrom. 39 (2024) 704–711, https://doi.org/10.1039/D3JA00421J.
[9] T.E. Lockwood, L. Schlatt, D. Clases, SPCal – an open source, easy-to-use processing platform for ICP-TOFMS-based single event data, J. Anal. At. Spectrom. 40 (2025) 130–136, https://doi.org/10.1039/D4JA00241E.
[10] I. Abad-Álvaro, E. Peña-Vázquez, E. Bolea, P. Bermejo-Barrera, J.R. Castillo, F. Laborda, Evaluation of number concentration quantification by single-particle inductively coupled plasma mass spectrometry: microsecond vs. millisecond dwell times, Anal. Bioanal. Chem. 408 (2016) 5089–5097, https://doi.org/10.1007/s00216-016-9515-y.
[11] F. Laborda, A.C. Gimenez-Ingalaturre, E. Bolea, J.R. Castillo, About detectability and limits of detection in single particle inductively coupled plasma mass spectrometry, Spectrochim. Acta Part B At. Spectrosc. 169 (2020) 105883, https://doi.org/10.1016/j.sab.2020.105883.
[12] J. Liu, K.E. Murphy, R.I. Maccuspie, M.R. Winchester, Capabilities of single particle inductively coupled plasma mass spectrometry for the size measurement of nanoparticles: *a* case study on gold nanoparticles, Anal. Chem. 86 (2014) 3405–3414, https://doi.org/10.1021/ac403775a.
[13] M.D. Montaño, H.R. Badiei, S. Bazargan, J.F. Ranville, Improvements in the detection and characterization of engineered nanoparticles using spICP-MS with microsecond dwell times, Environ. Sci. Nano 1 (2014) 338, https://doi.org/10.1039/C4EN00058G.
[14] J.W. Olesik, P.J. Gray, Considerations for measurement of individual nanoparticles or microparticles by ICP-MS: determination of the number of particles and the analyte mass in each particle, J. Anal. At. Spectrom. 27 (2012) 1143–1155, https://doi.org/10.1039/c2ja30073g.
[15] J. Fuchs, M. Aghaei, T.D. Schachel, M. Sperling, A. Bogaerts, U. Karst, Impact of the *p*article *d*iameter on *i*on cloud *f*ormation from gold *n*anoparticles in ICPMS, Anal. Chem. 90 (2018) 10271–10278, https://doi.org/10.1021/acs.analchem.8b02007.
[16] I. Kálomista, A. Kéri, D. Ungor, E. Csapó, I. Dékány, T. Prohaska, G. Galbács, Dimensional characterization of gold nanorods by combining millisecond and microsecond temporal resolution single particle ICP-MS measurements, J. Anal. At. Spectrom. 32 (2017) 2455–2462, https://doi.org/10.1039/c7ja00306d.
[17] A. Kéri, I. Kálomista, D. Ungor, Á. Bélteki, E. Csapó, I. Dékány, T. Prohaska, G. Galbács, Determination of the structure and composition of Au-Ag bimetallic spherical nanoparticles using single particle ICP-MS measurements performed with normal and high temporal resolution, Talanta 179 (2018) 193–199, https://doi.org/10.1016/j.talanta.2017.10.056.
[18] E. Bolea-Fernandez, D. Leite, A. Rua-Ibarz, T. Liu, G. Woods, M. Aramendia, M. Resano, F. Vanhaecke, On the effect of using collision/reaction cell (CRC) technology in single-particle ICP-mass spectrometry (SP-ICP-MS), Anal. Chim. Acta 1077 (2019) 95–106, https://doi.org/10.1016/j.aca.2019.05.077.
[19] A. Bazo, E. Bolea-Fernandez, A. Rua-Ibarz, M. Aramendía, M. Resano, Intensity- and time-based strategies for micro/nano-sizing via single-particle ICP-mass spectrometry: *a* comparative assessment using Au and SiO2 as model particles, Anal. Chim. Acta 1331 (2024) 343305, https://doi.org/10.1016/j.aca.2024.343305.
[20] L.A. Currie, Detection: *i*nternational update, and some emerging di-lemmas involving calibration, the blank, and multiple detection decisions, Chemom. Intell. Lab. Syst. 37 (1997) 151–181, https://doi.org/10.1016/S0169-7439(97)00009-9.
[21] L.A. Currie, On the detection of rare, and moderately rare, nuclear events, J. Radioanal. Nucl. Chem. 276 (2008) 285–297, https://doi.org/10.1007/s10967-008-0501-5.
[22] MARLAP, 20 *d*etection and *q*uantification, in: Multi-Agency Radiological Laboratory Analytical Protocols Manual, 2004. https://www.epa.gov/sites/default/files/2015-05/documents/402-b-04-001c-20_final.pdf.
[23] L.A. Currie, Limits for *q*ualitative *d*etection and *q*uantitative *d*etermination: *a*pplication to *r*adiochemistry, Anal. Chem. 40 (1968) 586–593, https://doi.org/10.1021/ac60259a007.
[24] F. Laborda, J. Jiménez-Lamana, E. Bolea, J.R. Castillo, Critical considerations for the determination of nanoparticle number concentrations, size and number size distributions by single particle ICP-MS, J. Anal. At. Spectrom. 28 (2013) 1220–1232, https://doi.org/10.1039/c3ja50100k.
[25] F. Laborda, J. Medrano, J.R. Castillo, Quality of quantitative and semiquantitative results in inductively coupled plasma mass spectrometry, J. Anal. At. Spectrom. 16 (2001) 732–738, https://doi.org/10.1039/b101814k.
[26] I.S. Begley, B.L. Sharp, Occurrence and reduction of noise in inductively coupled plasma mass spectrometry for enhanced precision in isotope ratio measurement, J. Anal. At. Spectrom. 9 (1994) 171–176, https://doi.org/10.1039/ja9940900171.